NANO LETTERS
Cite This: Nano Lett. 2018, 18, 669–674
Letter
pubs.acs.org/NanoLett

Merely Measuring the UV–Visible Spectrum of Gold Nanoparticles Can Change Their Charge State

Jose Navarrete,[†] Chris Siefe,[‡] Samuel Alcantar,[†] Michael Belt,[§] Galen D. Stucky,[†,∥] and Martin Moskovits*[,†]

[†]Department of Chemistry and Biochemistry, University of California Santa Barbara, Santa Barbara, California 93106, United States
[‡]Department of Materials Science and Engineering, Stanford University, 496 Lomita Hall, Stanford, California 94305, United States
[§]Department of Electrical and Computer Engineering, University of California Santa Barbara, Santa Barbara, California 93106, United States
[∥]Materials Department, University of California Santa Barbara, Santa Barbara, California 93106, United States

Supporting Information

ABSTRACT: Metallic nanostructures exhibit a strong plasmon resonance at a wavelength whose value is sensitive to the charge density in the nanostructure, its size, shape, interparticle coupling, and the dielectric properties of its surrounding medium. Here we use UV–visible transmission and reflectance spectroscopy to track the shifts of the plasmon resonance in an array of gold nanoparticles buried under metal-oxide layers of varying thickness produced using atomic layer deposition (ALD) and then coated with bulk layers of one of three metals: aluminum, silver, or gold. A significant shift in the plasmon resonance was observed and a precise value of ω_p, the plasmon frequency of the gold comprising the nanoparticles, was determined by modeling the composite of gold nanoparticles and metal-oxide layer as an optically homogeneous film of core–shell particles bounded by two substrates: one of quartz and the other being one of the aforementioned metals, then using a Maxwell-Garnett effective medium expression to extract ω_p for the gold nanoparticles before and after coating with the bulk metals. Under illumination, the change in the charge density of the gold nanoparticles per particle determined from the change in the values of ω_p is found to be some 50-fold greater than what traditional electrostatic contact electrification models compute based on the work function difference of the two conductive materials. Moreover, when using bulk gold as the capping layer, which should have resulted in a negligible charge exchange between the gold nanoparticles and the bulk gold, a significant charge transfer from the bulk gold layer to the nanoparticles was observed as with the other metals. We explain these observations in terms of the "plasmoelectric effect", recently described by Atwater and co-workers, in which the gold nanoparticles modify their charge density to allow their resonant wavelength to match that of the incident light, thereby achieving, a lower value of the chemical potential due to the entropy increase resulting from the conversion of the plasmon's energy to heat. We conclude that even the act of registering the spectrum of nanoparticles is at times sufficient to alter their charge densities and hence their UV–visible spectra.

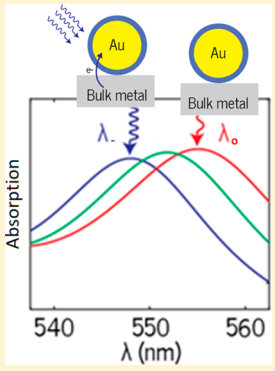

KEYWORDS: *Plasmonics, plasmoelectric effect, charge transfer, spectroscopy*

When illuminated with visible light, nanostructured noble metals exhibit a strong plasmon resonance.[1,2] The effect of size,[3,4] geometry,[2,5] surrounding medium,[6,7] and electrochemical charging,[8,9] on these resonances have beeen well documented and the agreement between experiment and theory is generally very good.[10] This tunability has allowed metal nanosystems to be fabricated with resonances matching the solar spectrum and subsequently used in plasmon mediated catalyis,[11−14] surface-enhanced Raman spectrosocopy,[15−17] and the development of plasmonic photovoltaics.[18,19] When metallic nanoparticles are placed in electrical contact with other materials, such as metal-oxides or metallic films, charge redistribution between the participating materials takes place, allowing their Fermi energies, which are measures of their chemical potentials, to equalize.[20−22] By choosing materials with either higher or lower Fermi energy levels relative to that of the nanoparticle, it is possible to charge the nanoparticle positively or negatively. Charge redistribution proportional to the difference in the work functions of nanoparticle and a contacting material has been shown experimentally.[23]

More recently, shifts in the plasmon resonance of metallic nanostructures due to the "plasmoeletric effect" an optically induced change in charge density were reported,[24,25] further expanding the possible strategies available for tuning the resonances of metallic nanostructures.

In this Letter, we report the optical properties of nanostructured media comprised of gold nanoparticles buried under nanolayers of dielectric (TiO_2, SiO_2, Al_2O_3) of varying

Received: June 19, 2017
Revised: December 27, 2017
Published: January 17, 2018

DOI: 10.1021/acs.nanolett.7b02592
Nano Lett. 2018, 18, 669–674

thickness with and without a backing layer of silver, aluminum, or gold. Because the resonances observed in the UV−vis spectrum depend on the multiple variables cited above, determining the charge state of the nanoparticles requires one to determine the plasmon frequency, ω_p, of the gold nanoparticles, which, in turn, required us to develop an appropriate model through which to extract this value. Accordingly, we developed an effective medium model in which the gold/dielectric phase is assumed to be a Maxwell-Garnett film comprised of core−shell particles and fitted the calculated UV−vis spectrum of this composite medium to what is observed, thereby determinig the medium's optical properties, including the value of ω_p of the gold nanoparticles that depends directly on the electron density.[26]

The results we obtained were remarkable on two accounts: first, the charge transfer from the metal bulk aluminum, silver, or gold layer to the gold nanoparticles (Au-NPs) turned out to be almost 2 orders of magnitude larger than what is predicted by traditional electrostatic models and approximately independent of the bulk metal's work function, and, second, bulk gold, which has a work function almost equal to that of the Au-NPs, nevertheless produced a very large charge transfer, even though the electrostatic model predicts zero charge transfer.[1,27] It is clear that the primary cause of our large observed charge transfer has little to do with work function differences and a wholly different mechanism must be sought. We propose that the large observed electron charge accumulation on the Au-NPs is due to the "plasmoelectric effect", an optically induced charge transfer mechanism, which is also based on equalizing the system's chemical potential, by additionally taking account of the entropy increase that occurs as a result of the increased heat dissipation of the system when in resonance with the light illuminating it. If so, it appears that under appropriate circumstance even low levels of illumination, such as those used in ordinary UV−visible spectroscopy, suffice to modify the charge density of metal nanoparticles. This could potentially impact broadly on the interpretation of certain UV−visible spectra of plasmonic nanoparticles.

The devices produced in this study were built on quartz substrates, using gold nanoparticles of varying dimensions with an average diameter of 10 nm embedded in one of three types of metal-oxide films of varying thickness deposited using atomic layer deposition (ALD), which in turn is backed by one of three bulk metal films, as shown schematically, in Figure 1. The optical properties of these assemblies were extracted at various stages of their construction from their UV−visible transmission or reflection spectra, and specifically the electron charge transferred from the metal layer to the Au-NPs was computed from the values of the plasma frequency of the gold nanoparticles, ω_p, returned by the fitting procedure. Close attention was also given to the electron scattering rate, γ, which is a measure of the metal's resisitivity that in turn depends on the nanoparticle's diameter (among other variables). This approach produced very good accord between the measured and computed transmittance and reflectance spectra of the composites, as shown in Figure 2.

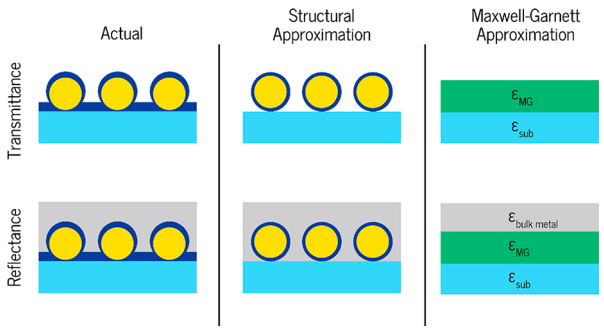

Figure 1. Schematic illustrating the approach used for approximating the optical constants of the gold/dielectric phase. Assuming the gold/dielectric phase to be a film of core−shell nanoparticles allows us to use the Maxwell-Garnett approximation to describe the optical constants of the film given by eq 1.

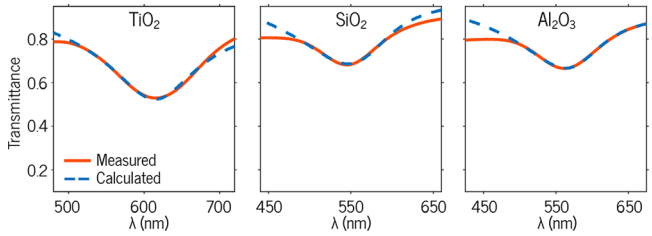

Figure 2. Measured and computed optical spectra of gold/dielectric phase with similar shell thicknesses, 2 nm for TiO_2 and Al_2O_3 and 1.5 nm for SiO_2. The calculated spectra were obtained by fitting our model for the fabricated films using least-squares emphasizing the spectral region in the neighborhood of the plasmon resonance.

Optical measurements were carried out on two types of devices: a two layer device (prior to the deposition of the bulk metal), shown in the top panel of Figure 1, and a three layer optical system, bottom panel of Figure 1. The substrate in both architectures is a quartz slide with dielectric constant ε_{sub}, on which the device is built. The gold nanoparticles with average radii ≈5 nm were produced by depositing a 2 nm mass thickness gold film on quartz using e-beam evaporation, then annealing the substrates at 500 °C for 10 min in nitrogen, causing the film to break up and form a two-dimensional random array of gold nanoparticles (Figure S1). These were then coated with one of three metal oxides (TiO_2, SiO_2, Al_2O_3) of varying thicknesses prepared by atomic layer deposition and confirmed by spectroscopic ellipsomtery on the metal-oxides deposited on a flat gold substrate. Transmittance measurements at normal incidence were carried out for the two layer device, and normal-incidence reflectance spectra were measured for the three-layer device following the deposition of a bulk layer of silver, aluminum, or gold by e-beam evaporation. All of the spectra were dominated by the surface plasmon resonance of the gold nanoparticles occurring in the 550 to 700 nm spectral range.

The spectra were fitted to the expression for the optical transmission through, or reflectance from a thin film of thickness $d = 2 \times r + t$, where $r = 5$ nm (radius of gold nanoparticle) and t is the layer thickness of metal-oxide deposited, residing on a quartz substrate. The optical constants of the film (as a function of wavelength) were assumed to be those of a Maxwell-Garnett effective medium film comprised of core−shell particles embedded either in air or in the bulk metal. The spectra were fitted using a Matlab-based least-squares program using standard thin-film on substrate optical formulas.[28]

The effective dielectric function, ε_{MG}, for the Maxwell-Garnett film composed of gold nanoparticles and the oxide coating as seen in Figure 1, is given by[29]

DOI: 10.1021/acs.nanolett.7b02592
Nano Lett. 2018, 18, 669−674

$$\varepsilon_{MG} = \varepsilon_m\left(\frac{1 + 2f_{cs}\beta}{1 - f_{cs}\beta}\right) \quad (1)$$

where ε_m is the dielectric function of the host media (air, silver, aluminum, or gold), f_{cs} is the volume fraction occupied by the core (ε_1)−shell (ε_2) particles within the host medium, and β, which is proportional to the polarizability, α, of the gold/dielectric core−shell particles is defined in the following equation[30,31]

$$\alpha = r^3\frac{(\varepsilon_2 - \varepsilon_m)(\varepsilon_1 + 2\varepsilon_2) + f(\varepsilon_1 - \varepsilon_2)(\varepsilon_m + 2\varepsilon_2)}{(\varepsilon_2 + 2\varepsilon_m)(\varepsilon_1 + 2\varepsilon_2) + f(2\varepsilon_2 - 2\varepsilon_m)(\varepsilon_1 - \varepsilon_2)} = r^3\beta \quad (2)$$

where ε_2 (the dielectric function of the metal-oxide shell) is assumed to be constant within the region of interest, and f is the ratio of the volume of the core to that of the entire core−shell particle. The fit algorithm adjusted the parameters contained in and therefore determined the best fit value for the dielectric function, ε_1, of the gold core from which we wish to extract the value of ω_p. The following function was assumed for ε_1 which contains among its adjustable parameters those we seek[31−33]

$$\varepsilon_1(\omega) = 1 - \frac{\omega_p^2}{\omega^2 + i\omega\gamma} + \sum_j^N \frac{a_j}{\omega_{0j}^2 - \omega^2 - i\omega\Gamma_j} + \varepsilon_\infty \quad (3)$$

This function consists of a drude term describing the contribution of the conduction electrons, a number of Lorentzians which together account for the contribution of interband transitions primarily to the UV−vis region of the spectrum and a constant accounting for the trailing contribution from transitions in the far UV. For bulk gold, the two parameters in the Drude term of eq 3 (the plasma frequency, ω_p, and γ the electron scattering rate), the parameters in the Lorentzians terms, and ε_∞ were determined by fitting eq 3 to the bulk gold optical constants measured by Johnson and Christy, Figure S2,[34] which yielded the values 9.1 and 0.0757 eV for ω_p and γ, respectively. The plasma frequency, ω_p, is related to the electron density in the nanoparticle, N, as follows[29]

$$\omega_p^2 = \frac{Ne^2}{m\varepsilon_0} \quad (4)$$

in which m is the effective mass of the electron, e is the electron charge, and ε_0 is the permittivity of free space.

Because of the very small sizes of the gold nanoparticles, a small change in the concentration of the electrons can have a significant effect on the plasma frequency, ω_p.[9] Fitting the transmission spectra (Figure S3) of bare gold nanoparticles deposited on quartz produced values of 8.99 and 0.281 eV for ω_p and γ, respectively, the former in close agreement with the reported plasma frequency of bulk gold, 9.1 eV. The slight descrepancy between the measured plasmon wavelength (530 nm) for the 10 nm diameter bare gold nanoparticles deposited on quartz compared to what one calculates (526 nm) for a single 10 nm diameter gold nanoparticle in vacuum is largely due to the effect of the quartz substrate. The smallness of the shift indicates minimal interparticle coupling.[35−37] The measured value of γ is larger than for bulk gold but reasonable for a 5 nm radius gold nanoparticle when the electrons scattering rate is corrected for the additional electron scattering at nanoparticle's boundaries using the expression, $\gamma = \gamma_B + A\frac{\nu_f}{R}$, where γ_B is the scattering rate for bulk gold, ν_f is the Fermi velocity for bulk gold, and A a geometric factor typically taken to be unity for a spherical particle.[31] This formula produces a value of 0.256 eV, in reasonable agreement with 0.281 eV the value obtained from the fit.

The transmission spectra obtained following the deposition of the metal-oxide shells of 2 nm TiO_2/Al_2O_3 or 1.5 nm SiO_2 on an array of gold nanoparticles supported on a quartz substrate are shown in Figure 2. As expected, the observed red shift of the wavelength at minimum transmittance tracks the index of refraction of the shell materials, n (SiO_2) = 1.5, n (Al_2O_3) = 1.7, n (TiO_2) = 2.4.[6] Using the above expressions (eqs 2−4), very good fits were obtained (Figure 2) which returned the following values: 9.0 eV for samples produced with TiO_2 and Al_2O_3 and 8.99 eV for the sample fabricated with SiO_2. The scattering rates were determined to be in the 0.350−0.480 eV range, somewhat higher than for the uncoated Au-NPs on the quartz slide. Samples with thicker shell layers for TiO_2, SiO_2, and Al_2O_3 were also measured. The results are reported in the Supporting Information as are the complete lists of the extracted optical parameters for all of our samples.

When gold nanoparticles are brought into contact with or in close proximity to bulk layers of other metals (in the absence of illumination), one normally expects charge transfer to occur to a degree and in a direction governed by the relative values of the work functions of the metals involved.[38] We carried out such experiments by depositing a bulk film of either silver or aluminum (and, subsequently, bulk gold) on the gold/dielectric material. The measured reflectance spectra were fit to a model which followed the strategy described above with the addition of a bulk layer of metal resident on the Maxwell-Garnett film's surface. The experimental results and the calculated reflectance spectra computed using the fitting parameters returning the best fit are shown in Figure 3. As stated previously, the

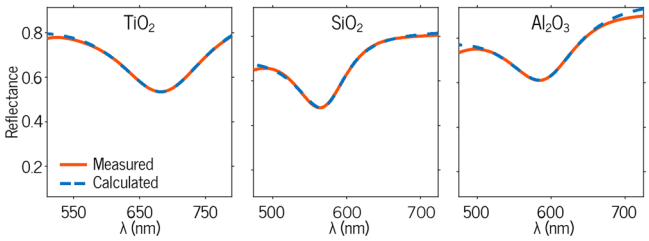

Figure 3. Measured and calculated reflectance spectra for core−shell nanoparticles with a silver bulk layer; an observed red shift λ_p with respect to the shell's corresponding transmittance spectra is observed due to various competing mechanisms. Shown spectra correspond to the equivalent shell thickness as those in Figure 2.

wavelength at the minimum transmittance (Figure 2) or maximum reflectance (Figure 3) cannot be used to determine the charge transfer that has occurred.[9,39] Only determining the values of ω_p produce meaningful values of the electron density in the gold nanoparticles. Assuming the effective electron mass is approximately unchanged by depositing the bulk metal the ratio of the electron density in the Au-NP after metal deposition to its value before is given by

$$\left(\frac{\omega_p'}{\omega_p}\right)^2 = \frac{N'}{N} \quad (5)$$

DOI: 10.1021/acs.nanolett.7b02592
Nano Lett. 2018, 18, 669−674

in which the primed variables refer to the values extracted from the reflectance spectra (Figure 3), whereas the unprimed values refer to numbers extracted from the transmission spectra (Figure 2) prior to the deposition of the bulk metal layer.

The extracted values (Table 1) show an increase in ω_p following the deposition of the bulk metal, implying an increased electron density in the gold nanoparticles, which, presumably were transferred from the bulk metal. But for the inordinately great magnitude of the electron density change, one might have presumed this net charge transfer arises from the process of equalizing the work functions between of gold nanoparticle and the bulk metal. We will show below that the charge transfer observed is far too large to be ascribed to work-function equalization alone.

Table 1. Extracted Optical Parameters and the Calculated Charge Transferred Per Gold Nanoparticle before (Unprimed) and after (Primed) the Addition of the Bulk Metal When Using 2 nm TiO_2/Al_2O_3 or 1.5 nm SiO_2

	bulk metal	ω_p (eV)	ω_p' (eV)	N'/N	e^- trans/NP
TiO_2	Al	9	11.5	1.64	19,598
	Ag	9	11.4	1.60	18,639
	Au	9	11.9	1.74	23,074
SiO_2	Al	8.9	10.39	1.36	11,189
	Ag	8.9	10.64	1.43	13,263
	Au	8.9	11.6	1.70	21,548
Al_2O_3	Al	9	10.2	1.28	8,771
	Ag	9	10.3	1.6	9,551
	Au	9	11	1.74	15,228

As illustrated in Figure 4 the trend in the magnitude of the charge transfer tracks the shell thickness, an understandable trend if one considers the shell to be a material of constant resistivity for all of the thicknesses used, generally a good assumption for atomic-layer deposited films.[40,41] Furthermore, the overall magnitude of the charge transfer also tracks the bulk electronic properties of the dielectrics used. TiO_2, a material with a high dielectric constant that is conductive due to oxygen vacancies present, allows a higher charge transfer from the bulk metal to the gold nanoparticles to occur. For the insulators, SiO_2 and Al_2O_3, there is a clear decrease in the magnitude of the charge transfer observed when using Al_2O_3 as the shell layer. We attribute this to the higher dielectric constant, bulk resistivity, and conduction band offsets of Al_2O_3 as compared to those of SiO_2.[42−44]

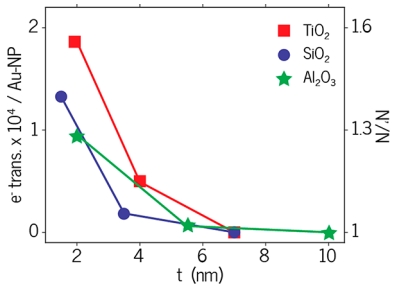

Figure 4. Calculated transfer of electrons per nanoparticle when in contact with a layer of bulk silver. The charge transfer trends with thickness of oxide deposited (t) as well as with the bulk electrical properties of the metal-oxide shell used with TiO_2 yielding the largest charge transfer due to its higher conductivity and high dielectric constant, whereas Al_2O_3 yields the lowest charge transfer due to its moderatelly higher dielectric constant than SiO_2 but with significantly lower electrical conductivity. The lines were not computed but function merely as a guide to the eye.

The most striking result noted in Table 1 is that the deposition of a bulk gold metal layer produces a charge transfer to the gold nanoparticles as large as or larger than those produced by the other two metals. Naively, one might conclude that the work function of the gold nanoparticles is larger than that of bulk gold. This, however, is not the case. Reported values for the work function or ionization values of gold nanoparticles indicate that for Au-NPs with radii ≈5 nm the work function is approximately equal to that of bulk gold.[45] We will show below that for the samples we produced the relatively large charge exchange between the bulk metal layer and the gold nanoparticles is negligibly impacted by the difference in work function. Instead, we propose that most of the charge exchange is the result of the so-called plasmo-electric effect, which successfully explains why charge transfer is obtained from gold nanoparticles to bulk gold despite the near equality of their work functions, and accounts for the very large charge transfers observed.

To justify the first statement which states that an electrostatics approach alone cannot account for the large changes in charge density of the gold nanoparticles, we calculated the expected number of electrons transferred from the bulk metal to the gold nanoparticles using methods developed by Peljo et al., who use the capacitance matrix approach to calculate the surface charge on particles of varying size and work functions.[46,47] The charges on two spherical conductors (q_i), A (Au-NP) and B (bulk metal sphere) of radii r_a and r_b, are computed by expressing the charges on each particle in terms of their outer electrostatic potentials (ψ_i) and the self-and mutual capacitances given as follows

$$\begin{bmatrix} q_a \\ q_b \end{bmatrix} = \begin{bmatrix} C_{AA} & C_{AB} \\ C_{AB} & C_{BB} \end{bmatrix} \begin{bmatrix} \psi_A \\ \psi_B \end{bmatrix} \tag{6}$$

where the elements in the matrix are as follows

$$C_{AA}(s) = C_0[\lambda(s) - \psi_0(x_b)] \tag{7}$$

$$C_{BB}(s) = C_0[\lambda(s) - \psi_0(x_a)] \tag{8}$$

$$C_{AB}(s) = -C_0[\lambda(s) + \gamma] \tag{9}$$

Here, $x_i = r_i/(r_a + r_b)$, $2\lambda(s) = \ln\{2r_a r_b/[(r_a + r_b)s]\}$, and $\psi_0(z) = d(\ln\Gamma(z))/dz$. Defining s as the distance between the two particles and assuming electrostatic equilibrium, the following holds

$$(\psi_B - \psi_A)_{eq} = \frac{-(\phi_B - \phi_A)}{e} \tag{10}$$

which implies the outer electrostatic potentials on each particle is dependent on the difference in their work functions (Figure 5).

The equations of Peljo et al., which relate to charge transfers between two metal spheres of differing metals and different radii, can be directly applies to our system, which consists of gold nanoparticles in contact with a bulk metal layer, by allowing the radius of one of the spheres to become very much larger than the radius of the other, that is, $r_b \gg r_a$, where sphere a is the gold nanosphere. Under such circumstances the surface potential of the gold nanoparticle after deposition of the bulk

DOI: 10.1021/acs.nanolett.7b02592
Nano Lett. 2018, 18, 669−674

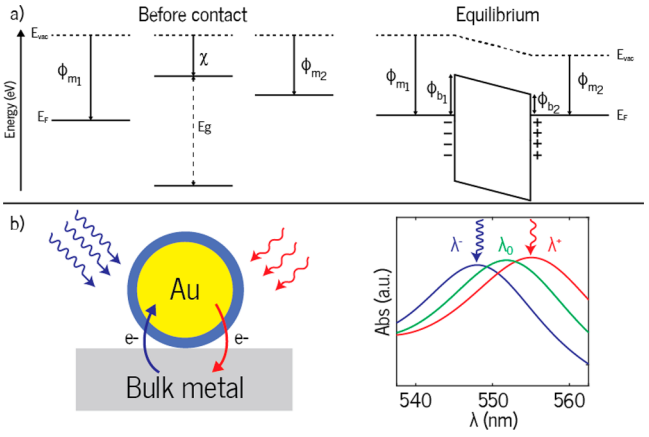

Figure 5. (a) Energy levels of participating materials where ϕ_{m1} is greater than ϕ_{m2} (i.e., gold core, ϕ_{m1}, and silver/aluminum bulk metals, ϕ_{m2}) with a dielectric layer of electron affinity χ before participating materials are brought into close proximity with each other and after contact causing the Fermi levels to equilibrate by redistributing of charge. (b) Schematic illustrating the plasmoelectric effect. When illuminated with photon wavelengths shorter (λ^-) than the natural resonance of the gold nanoparticle the nanoparticle accumulates charge, whereas if illuminated with photons of longer wavelength (λ^+) it will be depleted of charge. The sign on λ signifies the resulting optically induced charge of the nanoparticle as a result of the particle modifying its electron density to alter its resonance to match the wavelength of the incident photons.

metal layer will be approximately equal to the difference in the work functions of the materials, in other words, $\psi_A=\phi_A - \phi_B$, whereas the surface potential of the bulk metal will be zero, that is, $\psi_B \approx 0$. This implies that the relative shift of the Fermi level of the bulk metal will be negligible compared to the shift of Fermi level of the gold nanoparticle.[46] For our gold nanoparticles, ϕ_A = 5.3 eV and for the bulk silver metal approximated as a large sphere, ϕ_B = 4.3 eV with 2 nm TiO_2 shell and using eq 6, we compute that ≈400 electrons would be transferred per nanoparticle from the silver to the gold nanoparticles based on an electrostatic approximation, a significantly lower number than the 18,000 transferred electrons per gold nanoparticle (Table 1) determined from our measured values of ω_p.

Clearly, a model based on electrostatics alone cannot account for our observed results. We propose that the inordinate electron transfer we observe from the metal film to the gold nanoparticles is due to the action of the light illuminating our samples through the so-called plasmoelectric effect, a phenomenon predicted, observed, and named by Atwater and co-workers,[24,25] which also successfully accounts for our observation that an electron transfer of equivalent magnitude is also observed for gold nanoparticles in proximity to bulk gold.

Briefly, the plasmoelectric effect is an optically induced charging of nanostructured noble metals observed when a nanoparticle electrically connected to ground, such as nanoparticles residing on a transparent conductive oxide, alters its charge density so as to tune its resonance wavelength to the wavelength of the incident photon, when the light's wavelength is either slightly longer or shorter than the natural resonance wavelength of the gold particles. This arises from the fact that on resonance the system is at a lower free energy state, benefiting from the increased entropy resulting from the heat that is generated through nonradiative decay of the excited plasmon. Accordingly, if the incident light is of a shorter wavelength than that of the natural resonance wavelength of the nanoparticle, the nanoparticle will gain electrons from ground; if the illuminating light is of a longer wavelength than the resonance wavelength of the nanoparticle, electrons from the nanoparticle will flow to ground until its plasmon resonance wavelength matches the wavelength of the incident light. Moving electrons to and from a conducting nanoparticle to ground normally requires relatively little energy; hence charge transfer to or from a metallic particle illuminated by light slightly off plasmon resonance is likely, as predicted and reported by Atwater and co-workers.[24,25] By contrast, altering the structure of a strongly bound system such as a molecule so as to modify its electronic resonances would normally require a quantity of energy large enough so that its is likely not offset by the entropic effect; hence the equivalent process is not expected to be observed with most molecules.

One consequence of our proposal that what we observe is due to the plasmoelectric is the possibility that light of an intensity such as that normally used to measure UV−visible spectra would at times suffice to modify the charge density and hence the resonance condition of metal nanostructures. In general, one could see shifts due both to electrons moving from ground to the nanoparticle when the wavelength of the light is shorter than that of the particle's resonance and from the nanoparticle to ground when the NPs are illuminated with longer wavelengths than their resonance wavlengths. That in our experiment the process in which the charge transfer from ground to the nanoparticle is favored over the reverse process we ascribe to the unequal energies of the two Schottky barriers between the metals and the oxide shell, resulting in some degree of rectification.

The plasmoelectric effect was previously demonstrated with gold nanoparticles on FTO and gold hole-arrays on quartz.[24] In those reports the optically induced plasmoelectric effect yielded symmetrical surface charging about the natural resonance of the gold implying that when in direct contact with a conductive substrate serving as ground, the nanoparticles showed no net preference for either accumulating or depleting charge. The systems used in those experiments, however, are not structurally equivalent to ours. Referring to Figure 5, the potential barrier between the gold nanoparticle and the insulator (ϕ_{b1}) is larger than the barrier between the bulk metal and the insulator (ϕ_{b2}), which implies that over-the-barrier electron injection from the bulk metal to the gold nanoparticles is more probable due to the lower barrier.[48] Additionally, the results track reasonably well with the known bulk dielectric properties and electron conduction properties of TiO_2, SiO_2, and Al_2O_3.

In conclusion, using a Maxwell-Garnett effective medium approximation, we were able to extract reliable ω_p values of gold nanoparticles which served as the core in core−shell particles embedded in dielectric and bulk metal media. Because ω_p is a measure of the electron density of the nanoparticles, we determined that the proximity of a bulk metal (silver, aluminum, and gold) produced an increased negative charge on the gold core. The observed results could not be accounted for using traditional electrostatic arguments, which predict far too small a charge transfer than what is observed. However, our observations accorded well with what is predicted by the plasmoelectric effect, a phenomenon predicted and measured by Atwater and co-workers in which gold nanoparticles can acquire either positive or negative charges when illuminated by

DOI: 10.1021/acs.nanolett.7b02592
Nano Lett. 2018, 18, 669−674

light whose wavelength is near but not coincident with the natural plasmon resonance of the metal nanoparticle.

■ ASSOCIATED CONTENT

Supporting Information

The Supporting Information is available free of charge on the ACS Publications website at DOI: 10.1021/acs.nanolett.7b02592.

Comprehensive list of extracted optical parameters for the gold nanoparticles before and after bulk metal deposition as well as micrographs of gold nanoparticles before and after annealing (PDF)

■ AUTHOR INFORMATION

Corresponding Author

*E-mail: moskovits@chem.ucsb.edu.

ORCID

Jose Navarrete: 0000-0002-3650-3238

Galen D. Stucky: 0000-0002-0837-5961

Martin Moskovits: 0000-0002-0212-108X

Author Contributions

The manuscript was written through contributions of all authors. All authors have given approval to the final version of the manuscript.

Funding

This work was supported by the NSF PIRE-ECCI program (Advancing the U.S.-China partnership in electron chemistry and catalysis at interfaces, Grant OISE 09-68399). This work was supported by the Institute for Collaborative Biotechnologies through Grant W911NF-09-D-0001 from the U.S. Army Research Office. Use of the Shared Experimental Facilities of the Materials Research Science and Engineering Center at UCSB (MRSEC NSF DMR 1720256) is gratefully acknowledged. The UCSB MRSEC is a member of the NSF-supported Materials Research Facilities Network (www.mrfn.org).

Notes

The authors declare no competing financial interest.

■ ACKNOWLEDGMENTS

The authors are thankful to Dr. Dan Cohen and Wei Cao for their contributions towards the experimental procedure with the UV−vis spectrometer.

■ REFERENCES

(1) Kittel, C. *Solid State Physics*, 6th ed.; John Wiley & Songs, Inc.: New York, 1986.

(2) Mulvaney, P. *Langmuir* **1996**, *12*, 788−800.

(3) Daniel, M.-C.; Astruc, D. *Chem. Rev.* **2004**, *104*, 293−346.

(4) Link, S.; El-Sayed, M. a. *J. Phys. Chem. B* **1999**, *103*, 4212.

(5) Kamat, P. V. *J. Phys. Chem. B* **2002**, *106*, 7729−7744.

(6) Underwood, S.; Mulvaney, P. *Langmuir* **1994**, *10*, 3427−3430.

(7) Knight, M. W.; Wu, Y.; Lassiter, J. B.; Nordlander, P.; Halas, N. J. *Nano Lett.* **2009**, *9*, 2188−2192.

(8) Novo, C.; Funston, A. M.; Gooding, A. K.; Mulvaney, P. J. *J. Am. Chem. Soc.* **2009**, *131*, 14664−14666.

(9) Brown, A. M.; Sheldon, M. T.; Atwater, H. A. *ACS Photonics* **2015**, *2*, 459−464.

(10) Verbruggen, S. W.; Keulemans, M.; Martens, J. A.; Lenaerts, S. *J. Phys. Chem. C* **2013**, *117*, 19142−19145.

(11) Marimuthu, A.; Zhang, J.; Linic, S. *Science* **2013**, *339*, 1590−1593.

(12) Christopher, P.; Xin, H.; Linic, S. *Nat. Chem.* **2011**, *3*, 467−472.

(13) Watanabe, K.; Menzel, D.; Nilius, N.; Freund, H.-J. *Chem. Rev.* **2006**, *106*, 4301−4320.

(14) Mukherjee, S.; Libisch, F.; Large, N.; Neumann, O.; Brown, L. V.; Cheng, J.; Lassiter, J. B.; Carter, E. A.; Nordlander, P.; Halas, N. J. *Nano Lett.* **2013**, *13*, 240−247.

(15) Moskovits, M. *Rev. Mod. Phys.* **1985**, *57*, 783.

(16) Braun, G. B.; Lee, S. J.; Laurence, T.; Fera, N.; Fabris, L.; Bazan, G. C.; Moskovits, M.; Reich, N. O. *J. Phys. Chem. C* **2009**, *113*, 13622−13629.

(17) Wang, X.; Liu, Z.; Zhuang, M.-D.; Zhang, H.-M.; Wang, X.; Xie, Z.-X.; Wu, D.-Y.; Ren, B.; Tian, Z.-Q. *Appl. Phys. Lett.* **2007**, *91*, 101105.

(18) Mubeen, S.; Lee, J.; Lee, W. R.; Singh, N.; Stucky, G. D.; Moskovits, M. *ACS Nano* **2014**, *8*, 6066−6073.

(19) Atwater, H. A.; Polman, A. *Nat. Mater.* **2010**, *9*, 205−213.

(20) Zhang, Z.; Yates, J. T. *Chem. Rev.* **2012**, *112*, 5520−5551.

(21) Zhdanov, V. P. *Surf. Sci.* **2002**, *512*, L331−L334.

(22) Ioannides, T.; Verykios, X. E. *J. Catal.* **1996**, *161*, 560−569.

(23) Zhang, Y.; Pluchery, O.; Caillard, L.; Lamic-Humblot, A.-F.; Casale, S.; Chabal, Y. J.; Salmeron, M. *Nano Lett.* **2015**, *15*, 51−55.

(24) Sheldon, M. T.; van de Groep, J.; Brown, A. M.; Polman, A.; Atwater, H. a.; Van De Groep, J.; Brown, A. M. *Science* **2014**, *346*, 828−831.

(25) van de Groep, J.; Sheldon, M. T.; Atwater, H. A.; Polman, A. *Sci. Rep.* **2016**, *6*, 23283.

(26) Incel, A.; Güner, T.; Parlak, O.; Demir, M. M. *ACS Appl. Mater. Interfaces* **2015**, *7* (49), 27539−27546.

(27) Tonomura, O.; Sekiguchi, T.; Inada, N.; Hamada, T.; Miki, H.; Torii, K. *J. Electrochem. Soc.* **2012**, *159* (1), G1−G5.

(28) Tompkins, H. G. *Handbook of Ellipsometry*; Springer, 2005; Vol. *30*.

(29) Cai, W.; Shalaev, V. *Optical metamaterials: Fundamentals and applications*; Springer, 2010.

(30) Oldenburg, S. J.; Averitt, R. D.; Westcott, S. L.; Halas, N. J. *Chem. Phys. Lett.* **1998**, *288* (2−4), 243−247.

(31) Moskovits, M.; Srnová-Šloufová, I.; Vlčková, B. *J. Chem. Phys.* **2002**, *116* (23), 10435.

(32) Hergert, W. *The Mie Theory: Basics and Applications*; Imprint: Springer, 2012.

(33) Nehl, C. L.; Grady, N. K.; Goodrich, G. P.; Tam, F.; Halas, N. J.; Hafner, J. H. *Nano Lett.* **2004**, *4*, 2355−2359.

(34) Johnson, P. B.; Christy, R.-W. *Phys. Rev. B* **1972**, *6* (12), 4370.

(35) Atay, T.; Song, J. H.; Nurmikko, A. V. *Nano Lett.* **2004**, *4* (9), 1627−1631.

(36) Aubry, A.; Lei, D. Y.; Maier, S. A.; Pendry, J. B. *Phys. Rev. Lett.* **2010**, *105* (23), 2−5.

(37) Ghosh, S. K.; Pal, T. *Chem. Rev.* **2007**, *107* (11), 4797−4862.

(38) Yeo, Y.-C.; King, T.-J.; Hu, C. *J. Appl. Phys.* **2002**, *92* (12), 7266.

(39) Novo, C.; Funston, A. M.; Gooding, A. K.; Mulvaney, P. *J. Am. Chem. Soc.* **2009**, *131* (41), 14664−14666.

(40) Leskela, M.; Ritala, M. *Thin Solid Films* **2002**, *409* (1), 138−146.

(41) Jeong, C.-W.; Lee, J.-S.; Joo, S.-K. *Jpn. J. Appl. Phys.* **2001**, *40* (1R), 285.

(42) Afanas'ev, V. V.; Houssa, M.; Stesmans, A.; Heyns, M. M. *J. Appl. Phys.* **2002**, *91* (5), 3079.

(43) Bersch, E.; Rangan, S.; Bartynski, R. A.; Garfunkel, E.; Vescovo, E. *Phys. Rev. B: Condens. Matter Mater. Phys.* **2008**, *78* (8), 1−10.

(44) Stevanović, V.; Lany, S.; Ginley, D. S.; Tumas, W.; Zunger, A. *Phys. Chem. Chem. Phys.* **2014**, *16* (8), 3706−3714.

(45) Häberlen, O. D.; Chung, S.-C.; Stener, M.; Rösch, N. *J. Chem. Phys.* **1997**, *106* (12), 5189−5201.

(46) Holmberg, N.; Laasonen, K.; Peljo, P. *Phys. Chem. Chem. Phys.* **2016**, *18* (4), 2924−2931.

(47) Peljo, P.; Manzanares, J. A.; Girault, H. H. *Langmuir* **2016**, *32* (23), 5765−5775.

(48) Sze, S. M.. *Physics of Semiconductor Devices Physics of Semiconductor Devices*, 3rd ed.; John Wiley & Sons, 1995; Vol. *10*.

DOI: 10.1021/acs.nanolett.7b02592
Nano Lett. 2018, 18, 669−674